Characteristics of Thin-layer Infrared Drying of Green Bean

Ibrahim DOYMAZ, Azmi Seyhun KIPCAK and Sabriye PISKIN

Department of Chemical Engineering, Faculty of Arts and Science, Yildiz Technical University, Esenler, Istanbul, Turkey

Abstract

Doymaz I., Kipcak A.S., Piskin S. (2015): **Characteristics of thin-layer infrared drying of green bean**. Czech J. Food Sci., 33: 83–90.

The effect of infrared (IR) power on drying kinetics, rehydration, and colour of green beans was investigated. The drying experiments were carried out at 83, 104, 125, 146, 167, and 188 W. It is observed that drying characteristics, rehydration, and colour of bean slices were greatly influenced by infrared power. The drying data were fitted with five thin-layer drying models available in the literature. Results showed that Midilli et al. and Aghbashlo et al. models are superior to the other models for explaining the drying kinetics of green bean slices. Effective moisture diffusivity was calculated in the range of 6.57×10^{-10} to 4.49×10^{-9} m^2/s. Activation energy was estimated by a modified Arrhenius type equation and found to be 11.379 kW/kg.

Keywords: effective diffusivity; activation energy; infrared power; mathematical modelling

Bean (*Phaseolus vulgaris*) is a herbaceous annual plant of the family Leguminosae. Beans are a good source of carbohydrates, proteins, dietary fibre (mainly insoluble fibre), vitamins (thiamine, riboflavin, niacin, pyridoxine, and folic acid), and to a lesser extent certain minerals such as calcium, iron, copper, zinc, phosphorus, potassium, and magnesium, and the hull contains flavonoids, which function as antioxidants (Ulloa *et al.* 2013). The worldwide bean production in 2012 was 20 742 857 tons. The major producer countries include China, Indonesia, India, Turkey, Thailand, and Egypt. In Turkey green beans are grown on the area of 74 000 ha with production of 614 965 t in 2012 (FAO 2014). Due to the high initial moisture content green beans are very sensitive to microbial spoilage. Therefore, drying of the beans after harvesting is necessary in order to extend their storage life.

A drying process has been used for decades in food processing industries for efficient long-term preservation of final products. The basic objective in the drying of food products is the removal of water from fresh product reaching a level at which microbial spoilage is avoided (Calin-Sánchez *et al.* 2014). Hot air dying has many disadvantages such as lower energy efficiency, long drying times, but on the other hand it has been used widely (Feng &

Tang 1998; Pan *et al.* 2008a). Infrared (IR) heating has many advantages compared to the widely used hot air drying. High heat transfer coefficients, short process time, low cost of energy are the characteristic properties of IR. Since air is transparent to IR, the method can easily be applied at ambient air temperature. Also the equipment of IR can be compact with controllable parameters in order to control the overheating and fast heating (Sakai & Hanzawa 1994). In the IR, the used radiation impinges on the exposed fruit surfaces and penetrates to create internal heating with molecular vibration of the material, and the energy of radiation is converted into heat (Ginzburg 1969). The composition and structure of the fruit or vegetable along with the wavelength of IR determine the power of penetration. The electromagnetic wave energy is absorbed by the food as soon as it is exposed to IR radiation, and the studies report that the drying rate of the foods is higher compared to the hot air drying (Masamura *et al.* 1988). The IR method has been investigated for obtaining high-quality dried foodstuffs including fruits, vegetables, grains and the studies indicate that IR allows more uniform heating of foods with better quality (Sakai & Hanzawa 1994; Togrul 2006; Nowak & Lewicki 2004). Several researchers indicated favourable results for IR drying of stationary

and single kernel layers of rough rice (Abe & Afzal 1997; Pan *et al.* 2008a).

There are many studies where the IR method is used for the dehydration of several foods. Pan *et al.* (2008b) used sequential infrared radiation heating and freeze-drying for the purpose of banana dehydration, Das *et al.* (2009) studied the drying kinetics of high moisture paddy undergoing vibration-assisted IR drying, Afzal and Abe (2000) simulated the moisture change in barley during far-infrared radiation drying, Sharma *et al.* (2005) studied the thin-layer infrared radiation drying of onion slices. The effect of far-infrared drying on the water state and glass transition temperature in carrots was investigated by Xu *et al.* (2014), drying and conversion/degradation of isoflavones during infrared drying of soybean were investigated by Niamnuy *et al.* (2012), apple slices IR drying and onion slices IR and convective drying were studied by Nowak and Lewicki (2004) and Jain and Pathare (2004). However, there is no information available about infrared drying of green bean. In this study, the thin-layer drying behaviour of green bean in an infrared dryer was investigated, and mathematical modelling by using five thin-layer drying models available in the literature was performed. Also, the values of effective moisture diffusivity and activation energy were calculated.

MATERIAL AND METHODS

Sample. Fresh green beans (*Phaseolus vulgaris* L.) were purchased from a local market in Istanbul in March 2014 and kept in a refrigerator (1050T model; Arcelik, Eskisehir, Turkey) at 4°C prior to use. Before drying process, green beans were washed and sliced manually. The average length and thickness of a bean slice were 2 cm and 0.6 cm, respectively. The initial moisture content of the fresh bean was determined using the AOAC method (AOAC 1990), and found to be 9.89 ± 0.05 kg water/kg dry matter (DM).

Drying procedure. Drying experiments were carried out in a moisture analyser with one 250 W halogen lamp (Snijders Moisture Balance, Snijders b.v., Tilburg, the Netherlands). For the infrared drying process, the sample should be separated evenly and homogeneously over the entire pan. The drying experiments were performed at an infrared power level varying from 83 W to 188 W. The samples of green beans (approximately 25 ± 0.2 g) were removed from the dryer at time intervals of 10 min during the

drying process and their weights were recorded with a digital balance (BB3000 model; Mettler-Toledo AG, Grefensee, Switzerland), which has a sensitivity of 0.1 g. Drying was finished when the moisture content of samples was approximately 0.08 kg water/kg DM. The dried product was cooled and packed in low-density polyethylene bags. The experiments were triplicated and average values of the moisture content were used for drawing the drying curves.

Rehydration procedure. Dried samples at different IR power levels were rehydrated in water at 23°C for 360 minutes. About 4.0 ± 0.1 g dried samples were placed in glass beakers containing water at a ratio of 1 : 100 (w/w). At specified time as 360 min, the samples were then removed, blotted with tissue paper to eliminate excess water on the surface, and weighed with an electronic digital balance (model XB220A; Precisa Instruments AG, Dietikon, Switzerland) having a sensitivity of 0.001 g. The rehydration ratio (*RR*) was calculated according to Eq. (1):

$$RR = \frac{W_2 - W_1}{W_1} \qquad (1)$$

where: W_1 – weight of dried matter (g); W_2 – weight of material (g)

Colour evaluation. The colour values of the fresh and dried samples, at between 83 and 167 W IR power levels, were evaluated using a hand-held tristimulus colorimeter (CR-400 Chroma Meter; Konica Minolta, Osaka, Japan). The colour brightness coordinate L^* measures the whiteness value of a colour and ranges from black at 0 to white at 100. The chromaticity coordinate a measures red when positive and green when negative, and the chromaticity coordinate b^* measures yellow when positive and blue when negative (Celen & Kahveci 2013). For the colour determinations, five measurements were done, and the corresponding average and standard deviation were calculated for each set of green beans, fresh and dried at each infrared power.

Mathematical modelling. The experimental drying data obtained at different infrared power levels were fitted using five thin-layer drying models (Table 1). The moisture ratio (*MR*) of the sample was calculated using the following equation:

$$MR = \frac{M_t - M_e}{M_0 - M_e} \qquad (2)$$

where: M_t, M_0, M_e – moisture content at any time, initial moisture content, and equilibrium moisture content (kg water/kg DM), respectively; t – drying time (min)

The equilibrium moisture content (M_e) is relatively small compared with M_0, especially for infrared drying. Therefore, M_e was numerically set to zero in this study. So MR can be simplified to $MR = M_t/M_0$ (Calín-Sánchez *et al.* 2014; Chayjan & Shadidi 2014).

The drying rate *(DR)* was calculated using Eq. (3):

$$DR = \frac{M_t - M_{t+\Delta t}}{\Delta t} \tag{3}$$

where: $M_{t+\Delta t}$ – moisture content at $t+\Delta t$ (kg water/kg DM); t – time (min)

Statistical analysis. Data were analysed using Statistica 8.0.550 (StatSoft Inc., Tulsa, USA) software package. The parameters of models were estimated using a non-linear regression procedure based on the Levenberg-Marquardt algorithm. The fitting quality of the experimental data to all models was evaluated using the coefficient of determination (R^2), reduced chi-square (χ^2), and root mean square error (RMSE). The higher the R^2 value and lower values of χ^2 and RMSE, the better the fitness (Alibas 2014; Vega-Gálvez *et al.* 2014). The χ^2 and RMSE can be expressed as:

$$\chi^2 = \frac{\sum\limits_{i=1}^{N} (MR_{exp.i} - MR_{pre.i})^2}{N - z} \tag{4}$$

$$RMSE = \left[\frac{1}{N} \sum\limits_{i=1}^{N} (MR_{pre.i} - MR_{exp.i})^2 \right]^{1/2} \tag{5}$$

where: $MR_{exp,i}$, $MR_{pre,i}$ – experimental and predicted dimensionless moisture ratios, respectively; N – number of observations; z – number of constants

Determination of effective moisture diffusivity. Fick's second law of diffusion equation, symbolised as a mass-diffusion equation for drying of agricultural products in a falling rate period, is shown in the following equation:

$$\frac{\partial M}{\partial t} = \nabla [D_{eff} (\nabla M)] \tag{6}$$

Fick's second law of unsteady state diffusion given in Eq. (6) can be used to determine the moisture ratio in Eq. (7). The solution of the diffusion equation for infinite slab given by Crank (1975), and supposed uniform initial moisture distribution, negligible external resistance, constant diffusivity and negligible shrinkage, is:

$$MR = \frac{8}{\pi^2} \sum\limits_{n=0}^{\infty} \frac{1}{(2n+1)^2} \exp\left(-\frac{(2n+1)^2 \pi^2 D_{eff} t}{4L^2} \right) \tag{7}$$

where: D_{eff} – effective moisture diffusivity (m²/s); t – time (s); L – half-thickness of samples (m); n – positive integer

For longer drying periods, the above equation can be simplified to only the first term of the series, without much affecting the accuracy of the prediction.

$$MR = \frac{8}{\pi^2} \exp\left(-\frac{\pi^2 D_{eff} t}{4L^2} \right) \tag{8}$$

Rearranging Eq. (8), by application of logarithms, it can be expressed as a straight line of the form:

$$\ln(MR) = \ln\left(\frac{8}{\pi^2} \right) - \left(\frac{\pi^2 D_{eff}}{4L^2} t \right) \tag{9}$$

The effective moisture diffusivity is typically obtained by plotting $\ln(MR)$ versus drying time in Eq. (9), since the plot gives a straight line with a slope according to Eq. (10):

$$K = \frac{\pi^2 D_{eff}}{4L^2} \tag{10}$$

Computation of activation energy. Temperature is not a directly measurable variable in the IR power level during drying process in this study. For the calculation of activation energy, a modified form of the Arrhenius equation as derived by Dadali and Ozbek (2008) shows the relationship between the effective diffusivity and the infrared power level to sample weight.

$$D_{eff} = D_0 \exp\left(-\frac{E_a m}{P} \right) \tag{11}$$

where: D_0 – pre-exponential factor of the Arrhenius equation (m²/s); E_a – activation energy (W/kg); P – infrared power (W); m – sample weight (kg)

RESULTS AND DISCUSSION

Drying curves. The effect of infrared power on drying curves of green bean during drying is shown in Figure 1. The drying curves are typical of those for similar fruits and vegetables. It is apparent that the moisture content decreased steadily with drying time and decreased faster at higher infrared powers in all cases. The drying times required to reach the final moisture content of samples were 360, 200, 160, 100, 80, and 60 min at the infrared powers of 83, 104, 125, 146, 167, and 188 W, respectively. The average drying rate of samples increased 6 times, as the infrared power increased from 83 W to 188 W. As expected at a higher infrared power level the
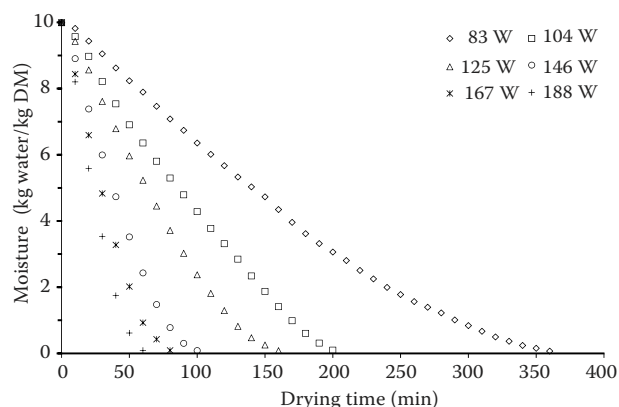
Figure 1. Drying curves of green bean slices at different IR power levels

Figure 2. Drying rate curves of green bean slices at different IR power levels

higher heat absorption resulted in higher product temperature, higher mass transfer driving force, faster drying rate and consequently shorter drying time (Kocabiyik & Tezer 2009; Ponkham *et al.* 2012; Ulloa *et al.* 2013).

Drying rate. The drying rate of the bean slices was calculated using Eq. (3). The changes in drying rates versus infrared powers are shown in Figure 2. The drying rate decreased continuously throughout the drying period. The absence of a period of constant drying rate was reported previously in many studies, where only the falling rate is present (Akhondi *et al.* 2011; Kayisoglu & Ertekin 2011). From Figure 2, the drying rates increased with the increasing infrared power levels. This means, heat and mass transfers at high powers are higher and the water loss is more excessive. During the drying process, drying rates were higher at the beginning of the process, and after that they decreased with a decrease of moisture content in the samples. The
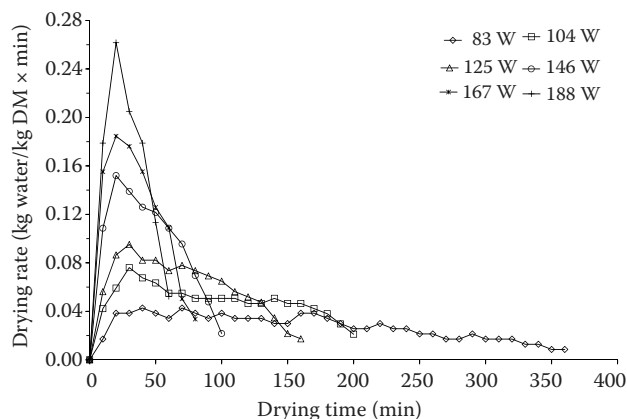
reason for a reduction of drying rate might be due to a reduction in the porosity of samples due to shrinkage with advancement, which increased the resistance to movement of water leading to a further fall in drying rates (Singh *et al.* 2006). The results were consistent with observations made by different authors on drying of various agricultural products (Kayisoglu & Ertekin 2011; Ponkham *et al.* 2012; Kumar *et al.* 2013; Sadin *et al.* 2014).

Rehydration characteristics. Rehydration is one of the important properties used to measure the quality of dried food materials (Lewicki 1998). It can also be considered as a measure of the injury caused by drying or treatment preceding drying. The results for the rehydration ratio were calculated from Eq. (1) and plotted against power levels, as shown in Figure 3. The rehydration ratio of samples dried at 188 W was higher than that of samples at all other power levels. An increase in the power level had an effect on the final rehydration ratio, which increased
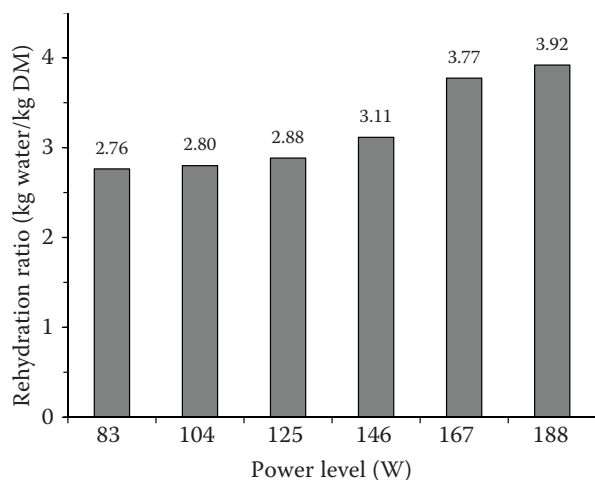

Figure 3. Rehydration ratio values of samples at different infrared power levels
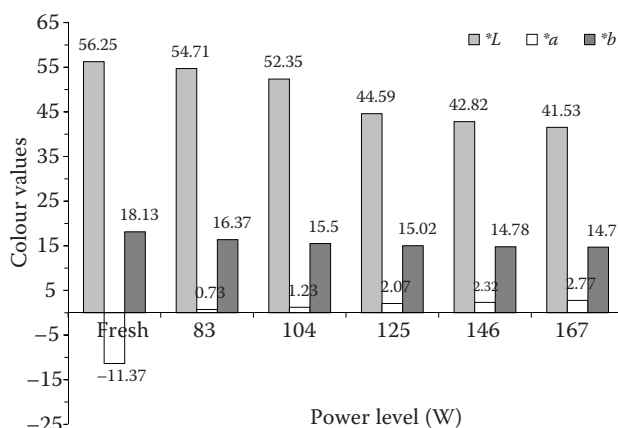

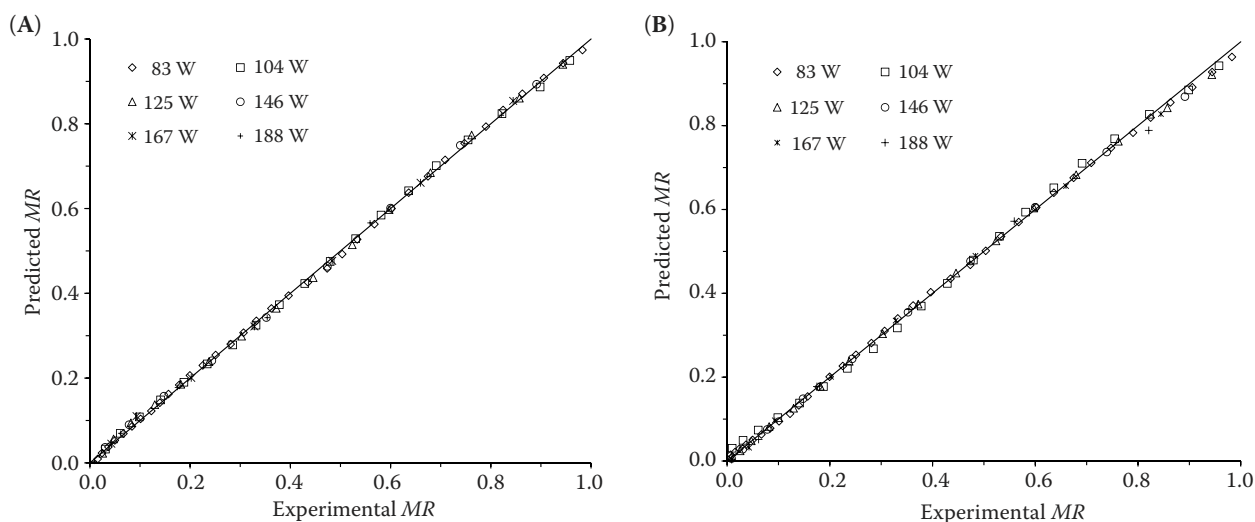Figure 4. Colour values of samples at different IR power levels

Figure 5. Comparison of experimental and predicted moisture ratio for green bean slice drying using the (**A**) Midilli et al. and (**B**) Aghbashlo et al. model

with the increasing power level (increasing product temperature).

Colour values. The results of the colour parameters fresh and obtained from the process of infrared drying are presented in Figure 4 for L^*, a^*, and b^*. Colour of fresh bean slices before processing is: L^* 56.25 ± 0.10; a^* −11.37 ± 0.05; b^* 18.13 ± 0.07. L^* values, which show the whiteness of the product, ranged between 56.25 and 41.53. It can be seen that the L^* value of dried product at 83 W is very similar to raw material. The lowest L^* value was evaluated for dried product at 188 W because of the Maillard reaction caused by a higher IR level and temperature. The differences in L^* values between the different drying processes of power levels were found statistically significant ($P < 0.05$). Significantly, the value of a product dried at different IR levels turned red due to the browning reaction during the drying process. Values a^* and b^* of dried products were found in the range of −11.37 to 2.77 and 14.70 to 18.13 for fresh and dried samples, respectively.

Models evaluation. Experimental results of *MR* variation with drying time were fitted to some thin-layer models as shown in Table 1. The best model was selected based on the highest R^2 and the lowest χ^2, and RMSE values. Results of the statistical computation are shown in Table 2. The R^2 values for all models were above 0.95. The statistical parameter estimations showed that R^2, χ^2, and RMSE values ranged from 0.9556 to 0.9996, 0.000034 to 0.007785, and 0.013343 to 0.303261, respectively. Among the thin-layer drying models, the Midilli et al. and Aghbashlo et al. models were found to represent the drying kinetics of green bean slices with high R^2 values and low χ^2, and RMSE values for all power levels. To validate the selected models, plots of experimental *MR* and predicted *MR* by Midilli et al. and Aghbashlo et al. models are shown in Figure 5.

Table 1. Models employed for fitting of experimental data

Models	Equation	Reference
Henderson and Pabis	$MR = a\exp(-kt)$	Chinenye *et al.* (2010)
Verma et al.	$MR = a\exp(-kt) + (1 - a)\exp(-gt)$	Togrul & Pehlivan (2004)
Weibull	$MR = \exp\left(-\left(\dfrac{t}{b}\right)^a\right)$	Corzo *et al.* (2008)
Midilli et al.	$MR = a\exp(-kt^n) + bt$	Balbay *et al.* (2013)
Aghbashlo et al.	$MR = \exp\left(-\dfrac{k_1 t}{1 + k_2 t}\right)$	Aghbashlo *et al.* (2009); Chayjan & Shadidi (2014)

a, b, c, g, k, k_1, k_2, n – empirical constants and coefficients in drying models

Table 2. Statistical results obtained from the selected drying models

Model	Power (W)								
	83			104			125		
	R^2	χ^2	RMSE	R^2	χ^2	RMSE	R^2	χ^2	RMSE
Henderson and Pabis	0.9662	0.003479	0.303261	0.9589	0.004342	0.243908	0.9604	0.004740	0.235963
Verma et al.	0.9923	0.000813	0.137621	0.9990	0.000111	0.029285	0.9914	0.001102	0.105147
Weibull	0.9953	0.000484	0.108935	0.9897	0.001084	0.121965	0.9951	0.000577	0.081431
Midilli et al.	0.9996	0.000034	0.026748	0.9994	0.000061	0.028286	0.9994	0.000076	0.026589
Aghbashlo et al.	0.9995	0.000046	0.030165	0.9984	0.000169	0.049545	0.9995	0.000053	0.015892
	146			167			188		
	R^2	χ^2	RMSE	R^2	χ^2	RMSE	R^2	χ^2	RMSE
Henderson and Pabis	0.9605	0.005456	0.203834	0.9634	0.005487	0.183231	0.9556	0.007785	0.186558
Verma et al.	0.9928	0.001116	0.082366	0.9946	0.000938	0.063962	0.9952	0.001043	0.081672
Weibull	0.9963	0.000513	0.059004	0.9975	0.000381	0.046387	0.9983	0.000307	0.032625
Midilli et al.	0.9993	0.000113	0.024384	0.9994	0.000119	0.019841	0.9996	0.000097	0.013847
Aghbashlo et al.	0.9995	0.000062	0.013343	0.9994	0.000077	0.018164	0.9984	0.000282	0.026927

Obviously, a good agreement was observed between experimental and predicted *MR* values. That is, the data points generally banded around a 45° straight line on the plots. This trend provides extra evidence for the suitability of the model to forecast the drying characteristics of green bean slices.

Effective moisture diffusivity. The natural logarithms of moisture ratio (ln *MR*) were plotted against drying time for different infrared powers. The determined values of the effective moisture diffusivity are shown in Figure 6 and were found to range between 6.57×10^{-10} and 4.49×10^{-9} m^2/s. It can be seen that D_{eff} values increased greatly with the increasing infrared power. This may be so because

the increase in infrared power caused a rapid rise in the temperature of green bean slices, which in turn increased the vapour pressure. As a result, it led to faster drying. Drying at 188 W has the highest value of effective moisture diffusivity and the lowest value was obtained for 83 W. The calculated effective diffusivity values are within the general range of 10^{-12} to 10^{-8} m^2/s for drying of agricultural products (Zogzas *et al.* 1996). These values are in fact consistent with those in literature, for example 1.08×10^{-9} to 6.70×10^{-9} m/s for hot-air drying of bean seeds (Resende *et al.* 2007), 9.3×10^{-11} to 1.06×10^{-9} m/s for convective drying of Lima bean (Da Silva *et al.* 2009), 1.2×10^{-10} to 3.2×10^{-10} m/s
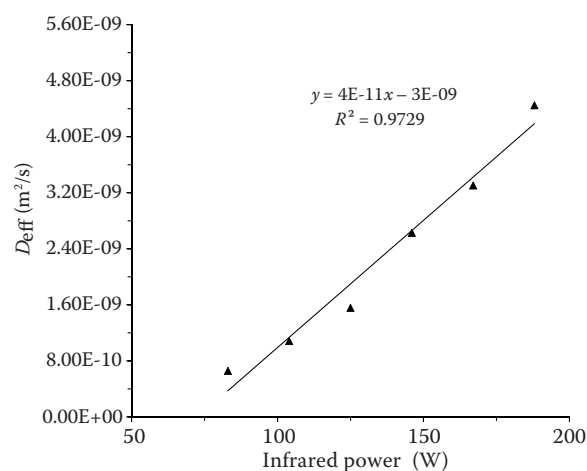
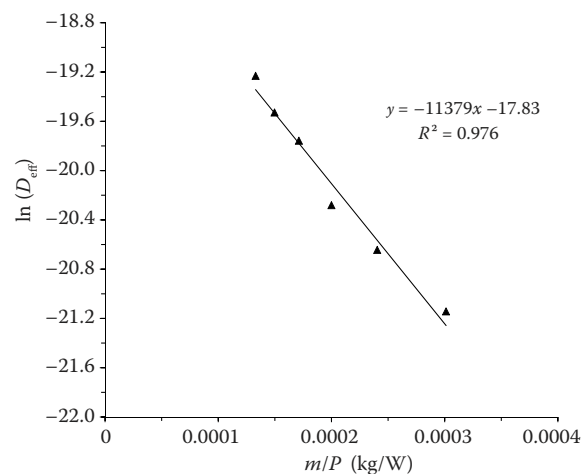Figure 6. Effective moisture diffusivity versus infrared levels

Figure 7. The Arrhenius-type relationship between effective moisture diffusivity and infrared levels

for vacuum drying of barbunya beans (Kayisoglu & Ertekin 2011), 3.04×10^{-9} to 2.64×10^{-8} m^2/s for fixed and semi-fluidised drying of Faba bean (Chayjan & Shadidi 2014), and 2.8×10^{-11} to 8.7×10^{-11} m/s for hot-air drying of fresh green bean (Abbasi Souraki & Mowla 2008). The effect of infrared power on effective moisture diffusivity is defined by the following equation:

$$D_{eff} = 4 \times 10^{-11}\, P - 2 \times 10^{-9} \qquad (R^2 = 0.9729) \quad (12)$$

Activation energy. The activation energy can be determined from the slope of Arrhenius plot, $\ln(D_{eff})$ versus m/P (Eq. 11). The $\ln(D_{eff})$ as a function of the sample weight/infrared power level was plotted in Figure 7. The slope of the line is $(-E_a)$ and the intercept equals to $\ln(D_0)$. The results show a linear relationship due to Arrhenius type dependence. Eq. (14) shows the effect of sample weight/power level on D_{eff} of samples with the following coefficients:

$$D_{eff} = 1.805 \times 10^{-8} \exp\left(-\frac{11379\,m}{P}\right) \quad (R^2 = 0.9760) \quad (13)$$

The estimated values of D_0 and E_a from modified Arrhenius type exponential Eq. (12) are 1.805×10^{-8} m^2/s and 11.379 kW/kg, respectively.

CONCLUSIONS

In this study, the drying characteristics of green beans were investigated in an infrared dryer at different infrared power levels. It can be seen that the drying time decreased with the increase in infrared power. The rehydration ratio of samples dried at 188 W was higher than that of samples at all other power levels. The colour quality of the product decreases significantly with the increase in infrared power. The constant-rate period was not observed from the drying curves. The drying process took place in the falling-rate period. To explain the drying curves of green bean, five thin-layer drying models were applied. The Midilli et al. and Aghbashlo et al. models gave the best results and showed a good agreement with experimental data obtained from the experiments. The effective moisture diffusivity was computed from Fick's second law, the values of which varied from 6.57×10^{-10} m^2/s to 4.49×10^{-9} m^2/s, over the infrared power range. Activation energy was estimated by a modified Arrhenius type equation and found to be 11.379 kW/kg.

References

Abbasi Souraki B., Mowla D. (2008): Drying behavior of fresh green beans in an inert medium fluidized bed. Journal of Food Processing and Preservation, 32: 697–718.

Abe T., Afzal T.M. (1997): Thin-layer infrared radiation drying of rough rice. Journal of Agricultural Engineering Research, 67: 289–297.

Afzal T.M., Abe T. (2000): Simulation of moisture changes in barley during far infrared radiation drying. Computers and Electronics in Agriculture, 26: 137–145.

Aghbashlo M., Kianmehr M.H., Khani S., Ghasemi M. (2009): Mathematical modeling of carrot thin-layer drying using new model. International Agrophysics, 23: 313–317.

Akhondi E., Kazemi A., Maghsoodi V. (2011): Determination of a suitable thin layer drying curve model for saffron (*Crocus sativus* L.) stigmas in an infrared dryer. Scientia Iranica, 18: 1397–1401.

Alibas I. (2014): Microwave, air and combined microwave-air drying of grape leaves (*Vitis vinifera* L.) and the determination of some quality parameters. International Journal of Food Engineering, 10: 69–88.

AOAC (1990): Official Method of Analysis. Association of Arlington, Official Analytical Chemists.

Balbay A., Sahin O., Ulker H. (2013): Modeling of convective drying kinetics of pistachio kernels in a fixed bed drying system. Thermal Science, 17: 839–846.

Calín-Sánchez A., Figiel A., Wojdylo A., Szaryez M., Carbonell-Barrachina A.A. (2014): Drying of garlic slices using convective pre-drying and vacuum-microwave finishing drying: Kinetics, energy consumption, and quality studies. Food and Bioprocess Technology, 7: 398–408.

Chayjan R.A., Shadidi B. (2014): Modeling high-moisture faba bean drying in fixed and semi-fluidized bed conditions. Journal of Food Processing and Preservation, 38: 200–211.

Celen S., Kahveci K. (2013): Microwave drying behaviour of tomato slices. Czech Journal of Food Sciences, 31: 132–138.

Chinenye N.M., Ogunlowo A.S., Olukunle O.J. (2010): Cocoa bean (*Theobroma cacao* L.) drying kinetics. Chilean Journal of Agricultural Research, 70: 633–639.

Corzo O., Bracho N., Pereira A., Vásquez A. (2008): Weibull distribution for modelling air drying of coroba slices. LWT- Food Science and Technology, 41: 2023–2028.

Crank J. (1975): The Mathematics of Diffusion. London, Oxford University Press.

Da Silva W.P., Precker J.W., De Lima A.G.B. (2009): Drying kinetics of Lima bean (*Phaseolus lunatis* L.) experimental determination and prediction by diffusion models. International Journal of Food Engineering, 5(3): Article 9.

Dadali G., Ozbek B. (2008): Microwave heat treatment of leek: drying kinetic and effective moisture diffusivity. International Journal of Food Science & Technology, 43: 1443–1451.

Das I., Das S.K., Bal S. (2009): Drying kinetics of high moisture paddy undergoing vibration-assisted infrared (IR) drying. Journal of Food Engineering, 95: 166–171.

FAO (2014): FaoStat: Agriculture data. Available at http://faostat.fao.org/site/567/DesktopDefault.aspx?PageID=567#ancor (acessed Feb 07, 2014).

Feng H., Tang J. (1998): Microwave finish drying of diced applies in a spouted bed. Journal of Food Science, 63: 679–683.

Ginzburg A.S. (1969): Application of Infrared Radiation in Food Processing. London, Leonard Hill.

Jain D., Pathare B. (2004): Selection and evaluation of thin layer drying models for infrared radiative and convective drying of onion slices. Biosystems Engineering, 89: 289–296.

Kayisoglu S., Ertekin C. (2011): Vacuum drying kinetics of barbunya bean (*Phaseolus vulgaris* L. *elipticus* Mart.). The Philippine Agricultural Scientist, 94: 285–291.

Kocabiyik H., Tezer D. (2009): Drying of carrot slices using infrared radiation. International Journal of Food Science & Technology, 44: 953–959.

Kumar A., Singh M., Singh G. (2013): Effect of different pretreatments on quality of mushrooms during solar drying. International Journal of Food Science & Technology, 50: 165–170.

Lewicki P.P. (1998): Some remarks on rehydration of dried foods. Journal of Food Engineering, 36: 81–87.

Masamura A., Sado H., Honda T., Shimizu M., Nabethani H., Hakajima M. (1988): Drying of potato by far infrared radiation. Nippon Shokuhin Kogyo Gakkaishi, 35: 309–314.

Niamnuy C., Nachaisin M., Poomsa-Ad N., Devahastin S. (2012): Kinetic modelling of drying and conversion/degradation of isoflavones during infrared drying of soybean. Food Chemistry, 133: 946–952.

Nowak D., Lewicki P.P. (2004): Infrared drying of apple slices. Innovative Food Science and Emerging Technologies, 5: 353–360.

Pan Z., Khir R., Godfrey L.D., Lewis R., Thompson J.R., Salim A. (2008a): Feasibility of simultaneous rough rice drying and disinfestations by infrared radiation heating and rice milling quality. Journal of Food Engineering, 84: 469–479.

Pan Z., Shih C., McHugh T.H., Hirschberg E. (2008b): Study of banana dehydration using sequential infrared radiation heating and freeze-drying. LWT-Food Science and Technology, 41: 1944–1951.

Ponkham K., Meeso N., Soponronnarit S., Siriamornpun S. (2012): Modeling of combined far-infrared radiation and air drying of a ring shaped-pineapple with/without shrinkage. Food and Bioproducts Processing, 90: 155–164.

Resende O., Corrêa P.C., Jarén C., Moure A.J. (2007): Bean moisture diffusivity and drying kinetics: a comparison of the liquid diffusion model when taking into account and neglecting grain shrinkage. Spanish Journal of Agricultural Research, 5: 51–58.

Sadin R., Cheigini G.R., Sadin H. (2014): The effect of temperature and slice thickness on drying kinetics tomato in the infrared dryer. Heat and Mass Transfer, 50: 501–507.

Sakai N., Hanzawa T. (1994): Application and advances in far infrared heating in Japan. Trends in Food Science & Technology, 5: 357–362.

Sharma G.P., Verma R.C., Pathare P.B. (2005): Thin-layer infrared radiation drying of onion slices. Journal of Food Engineering, 67: 361–366.

Singh B., Panesar P.S., Nanda V. (2006): Utilization of carrot pomace for the preparation of a value added product. World Journal of Dairy & Food Sciences, 1: 22–27.

Togrul H. (2006): Suitable drying model for infrared drying of carrot. Journal of Food Engineering, 77: 610–619.

Togrul I.T., Pehlivan D. (2004): Modelling of thin layer drying kinetics of some fruits under open-air sun drying process. Journal of Food Engineering, 65: 413–425.

Ulloa J.A., Bonilla-Sánchez C.R., Ortíz-Jiménez M.A., Rosas-Ulloa P., Ramírez-Ramírez J.C., Ulloa-Rangel B.E. (2013): Rehydration properties of precooked whole beans (*Phaseolus vulgaris*) dehydrated at room temperature. CyTA – Journal of Food, 11: 94–99.

Vega-Gálvez A., Puente-Díaz L., Lemus-Mondaca R., Miranda M., Torrres M.J. (2014): Mathematical modelling of thin-layer drying kinetics of Cape gooseberry (*Physalis peruviana* L.). Journal of Food Processing and Preservation, 38: 728–736.

Xu C., Li Y., Yu H. (2014): Effect of far-infrared drying on the water state and glass transition temperature in carrots. Journal of Food Engineering, 136: 42–47.

Zogzas N.P., Maroulis Z.B., Marinos-Kouris D. (1996): Moisture diffusivity data compilation in foodstuffs. Drying Technology, 14: 2225–2253.

Corresponding author:

Dr Azmi Seyhun Kipcak, Yildiz Technical University, Faculty of Arts and Science, Department of Chemical Engineering, 34210 Esenler, Istanbul, Turkey; E-mail: skipcak@yildiz.edu.tr/seyhunkipcak@gmail.com